Supercond. Sci. Technol. 8 (1995) 214–218. Printed in the UK

Orientation of Y_2BaCuO_5 precipitates during unidirectional solidification of $Y_1Ba_2Cu_3O_{7-\delta}$ under a magnetic field

L Durand†, F Kircher‡, P Régnier†, D Chateigner‖, N Pellerin§, F J Gotor§, P Simon§ and P Odier§

† CEA/CE Saclay/CEREM/SRMP, 91 191 Gif sur Yvette, France
‡ CEA/CE Saclay/DSM/DAPNIA, 91 191 Gif sur Yvette, France
§ CRPHT-CNRS, 45 071 Orléans Cedex 2, France
‖ Laboratoire de Cristallographie Associé à l'Université Joseph Fourier, CNRS, 38 042 Grenoble Cedex, France

Received 12 January 1995

Abstract. The effect of a vertical magnetic field on Y_2BaCuO_5 (211) precipitates during horizontal unidirectional solidification of YBaCuO has been investigated. EPR shows first that some of the residual 211 particles are not randomly oriented in the 123 matrix when the sample is processed under a magnetic field. Secondly, the analysis of the angular dependency of the EPR spectra shows that these particles tend to be oriented in the 123 crystal with their b_{211} crystallographic axis parallel to the applied magnetic field and also to the c_{123} axis. X-ray pole figures on the same sample lead to an identical conclusion. The consequences of this observation regarding $YBa_2Cu_3O_{7-\delta}$ (123) crystallization are discussed.

1. Introduction

The melt texture growth processing based on a directional solidification is successful in overcoming the weak link problem in bulk YBaCuO superconductors [1–4]. Unfortunately, application of a thermal gradient alone is not sufficient to align the 123 a–b planes of the grains parallel to it. However, experiments on 123 particles at room temperature [5, 6] demonstrate that the c_{123} axis of the grains can be oriented parallel to the applied magnetic field, due to the anisotropy of the magnetic susceptibility of YBaCuO in the paramagnetic state. To benefit from this remarkable property, de Rango *et al* [7] decided to apply a magnetic field during an MTG process. They discovered that a vertical magnetic field induces an alignment of the C_{123} axis parallel to it and hence puts the a–b planes horizontal, resulting in the growth of fibres of high J_c [8].

However, in a large part of the high temperature thermal treatment, $YBa_2Cu_3O_{7-\delta}$ (123) is no longer stable but instead transforms into Y_2BaCuO_5 plus a peritectic liquid. Because of incomplete recombination between primary 211 and the liquid upon cooling, residual 211 particles are left as inclusions. Hence the origin of the magnetic field effect is not clear: does it act on the melt before solidification or on stable nuclei? Moreover, controlling the 211 size distribution in the melt is one of the key factors for growing large 123 crystals [9–12]. In addition, it is known that those trapped particles enhance the superconducting properties because of indirect pinning of vortices [4, 13–15].

The possible orientation relations between 211 and 123 are of great interest, both for understanding the mechanisms of solidification and possibly for improving superconducting properties. The usual model for normal melt texturing (without any applied magnetic field) is a random orientation of 211 in the 123 crystal [4]. Only a few reports recognize possible relations between 211 and 123 by TEM [12, 14, 16]. However, Pellerin *et al* [17] have shown non-isotropic directional distributions of 211 particles in modified MTG textured YBaCuO by using EPR measurements. Based on the silent EPR behaviour of Cu in cuprates [18, 19] and on the anisotropic signal of Cu^{2+} in 211 [20], EPR allows us to study the statistical orientation of 211 particles inside a 123 single domain.

In this paper we report on the characterization of 211 inclusions by EPR spectroscopy and X-ray pole figures in YBCO samples prepared with or without magnetic field during unidirectional solidification.

2. Experimental details

A powder of 123 + 20% in weight of 211 was prepared by the sol-gel technique [21]. It was tested by X-ray diffraction and differential scanning calorimetry. It was very pure with respect to the presence of unreacted copper phases as proved by an unique melting event starting at 1022 °C in oxygen, figure 1. Note that the addition of 211 phase lowers the onset temperature of the melting and widens it, as already observed elsewhere [22].

0953-2048/95/040214+05$19.50

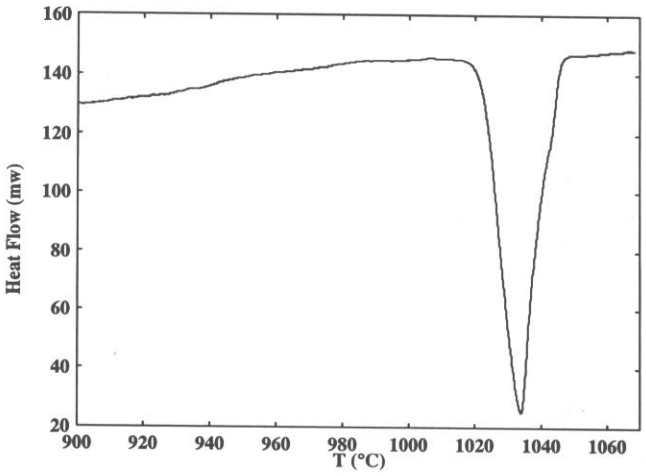

Figure 1. DSC thermogram of the 123 + 20 wt.% 211 powder used in this study. The absence of melting events below the peritectic decomposition (onset at 1022 °C) is an indication of high purity of the powder.

After calcination at 875 °C for 12 h in air, pellets of this powder were uniaxially pressed at 100 MPa and sintered at 930 °C for 10 h in air. Bars ($20 \times 5 \times 5$ mm^3) were then cut from the sintered ceramics and placed in the texturing furnace.

The set-up consisted in a horizontal tubular furnace equipped with a pulling system. This device was placed in a superconducting magnet generating a vertical magnetic field of 4 tesla. The magnetic field was constant over 30 cm in the middle of the furnace, which was much more than the sample length (about 5 cm).

The precursor bars were positioned on regularly spaced (every 4 mm) MgO single crystalline bars, in such a way that their long axes were collinear with the furnace axis. The whole system was placed in the middle of the furnace, where the thermal gradient was flat (less than 1 °C cm^{-1}). The experimental procedure is schematized in figure 2. After 1 h annealing at the sintering dwell, the temperature was quickly raised (600 °C h^{-1}) up to 1150 °C so as to melt the sample. It was held for 6 min and then cooled down to 1060 °C which is about 40 °C above the temperature range where the peritectic recrystallization can start. After 1 h at this temperature for homogenizing the melt, the sample was rapidly transferred to a cooler zone where the temperature gradient was 30 °C cm^{-1} so as to cool it unidirectionally. The sample was then very slowly pulled from this position (1 mm h^{-1}) towards the furnace entrance. When its hot end reached 900 °C all the sample was solidified and the furnace was rapidly cooled (at a rate of 20 °C h^{-1}). The experiments were performed in flowing oxygen. The application of the magnetic field was totally independent of all other parameters controlling the thermal cycle.

Two types of samples were elaborated: sample A was prepared with the magnetic field applied before melting of the sample and until the end of solidification; sample B was prepared identically but without applying the magnetic field.

The texture of both 123 and 211 phases in sample A were investigated by pole figures measurements using x-ray diffraction in the Schulz reflection geometry [23].

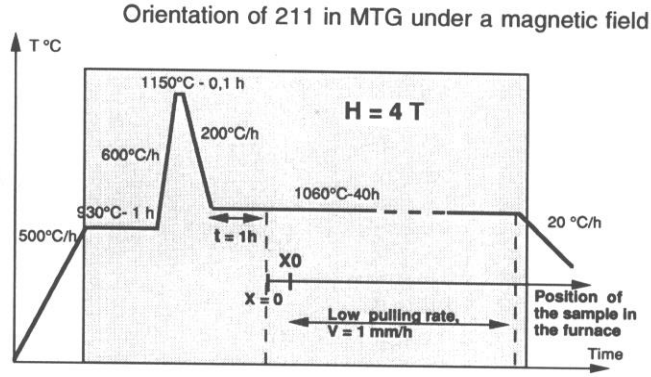

Figure 2. Thermal cycle applied to the sample during unidirectional solidification. For sample A a magnetic field of 4 T has been applied before melting of the sample until the end of solidification.

Experimental set-up [24] and data corrections [25] are detailed elsewhere.

Small pieces of single domains (about $1 \times 2 \times 0.5$ mm^3) were obtained by cleavage along the a–b planes for EPR analysis. The spectra were recorded on an X-band Bruker ER200D-SRC spectrometer (microwave frequency 9.7 GHz) operating at room temperature. The angle between the c_{123} axis and the static magnetic field could be varied between known values.

3. Results

Samples A and B both exhibited a single domain of about 15 mm in length and 4×4 mm^2 square section. Texture analysis of sample A was performed on a face perpendicular to the applied magnetic field. Figure 3(a) shows one intense $\{005\}_{123}$ pole at the centre of the pole figure. The dispersion of this pole is only 5° at half full maximum intensity, and consequently reaches a high pole density value of 1130 mrd (multiple of random distribution of crystallites). The four other poles present at 15% of I_{max} are indexed by the $\{104/014\}_{123}$ reflections (present at the same Bragg angle position as $\{005\}_{123}$) and reveal a three-dimensional texture character. In sample B, analysed on the same type of face as sample A, the c_{123} axis is at 75° from the perpendicular to this face. We can conclude that the applied magnetic field has greatly favoured the c_{123} alignment.

Figure 3(b) presents the central zone of the $\{040\}_{211}$ pole figure ($-15° \leq \lambda \leq 15°$) of sample A. It evidences a preferential orientation of 211 crystallites. The $\{040\}_{211}$ pole is extended by approximately 20°C, while there remains a proportion of 211 phase randomly oriented (constant diffracted signal over the entire pole figure). However, overlapping of $\{040\}_{211}$ with $\{115\}_{123}$ diffraction peak prevent us getting the genuine pole density of $\{040\}_{211}$.

The EPR measurements on the textured samples are presented in figure 4. Figure 4(a) shows a typical spectrum of a pure 211 powder. It shows two features of which the positions are characteristic of the Landé factor, g, a tensor which fixes the magnetic field position of the EPR lines through the relation, $h\nu = \beta HgS$ (where H and S are respectively the magnetic field and the spin vectors). For a free electron, $g = 2.0023$. The values found, 2.222 and 2.07, are typical of a Cu^{2+} ion in a non-symmetrical

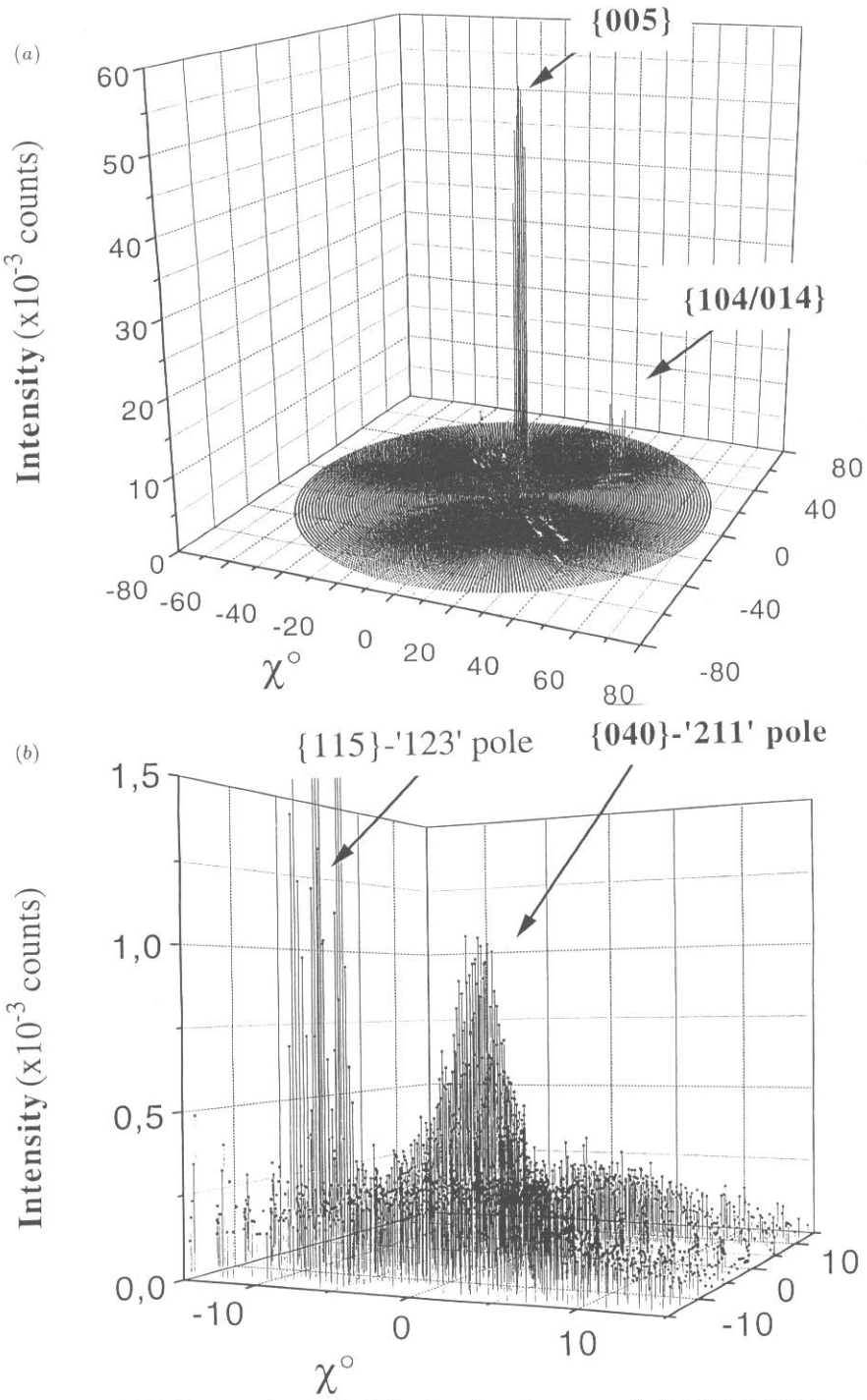

Figure 3. Pole figures of sample A (textured under magnetic field); (*a*) {005} pole of 123; (*b*) {040} pole of 211.

symmetry site. They respectively correspond to the values $g_{\parallel}$ and $g_{\perp}$ of the g tensor of the Cu^{2+}, i.e. spin 1/2, in the local orthorhombic site imposed by the crystallographic symmetry of 211 [20]. In this structure, the g tensor coincides with the crystallographic axis a_{211}, b_{211} and c_{211} ($a_{211} = 0.5658$ nm, $b_{211} = 0.7132$ nm, $c_{211} = 1.2181$ nm), i.e. g_x with a_{211}, g_y with c_{211} and g_z with b_{211}. The splitting $g_x - g_y$ being small, we use $g_{\perp}$ for the mean arithmetic value of g_x and g_y, while $g_{\parallel}$ corresponds to g_z. This powder does not present any angular dependency when rotating the sample in the spectrometer as expected. Figure 4(*b*) shows the same spectrum recorded for sample A solidified under a thermal gradient plus a magnetic field perpendicular to it. The angular dependency of the spectrum has been studied and, for the sake of simplicity, only two orientations are reported here. In this figure (H, c_{123}) denotes the angle between the static magnetic field of the spectrometer and c_{123}. There is an obvious strong orientation effect of

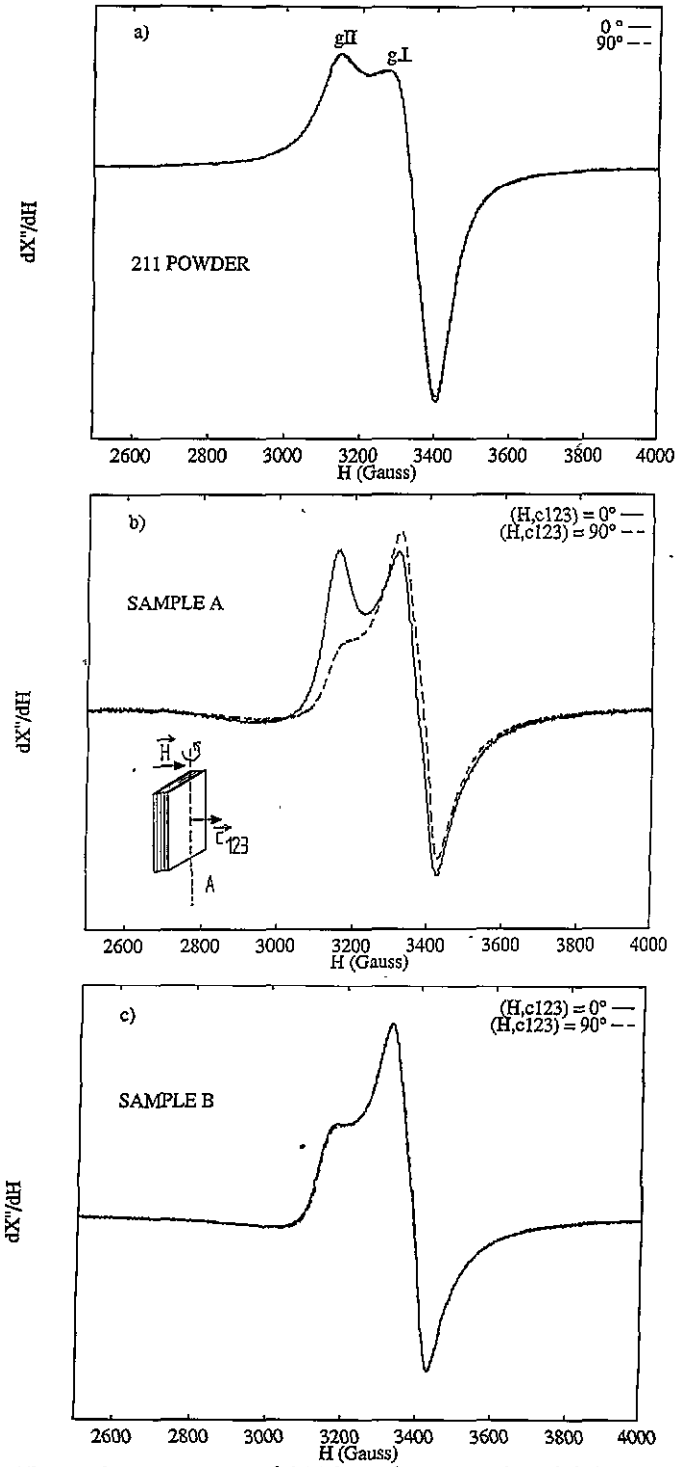

Figure 4. EPR spectra of 211 in various samples: (*a*) 211 powder; (*b*) sample A: YBaCuO melt-textured under a magnetic field; (*c*) sample B: YBaCuO melt-textured without a magnetic field. (H, c_{123}) denotes the angle between the static magnetic field of the EPR spectrometer and the direction of the c_{123} axis of the single domain analysed.

211 particles. The same experiment has been repeated for sample B, reported in figure 4(*c*). Sample B was prepared only under a thermal gradient; no magnetic field was applied. Clearly, due to a random orientation of the 211 particles there is no angular dependency.

The differences between spectra 4(*a*) and 4(*c*) are due to a non-negligible conductivity of the textured sample B compared with the pure 211 powder. It induces an absorption effect superimposed on the signal which can be reduced to practically zero by de-oxygenating the sample in Ar at 600 °C for 48 h. In such a case the normal shape of the 211 powder spectrum is restored in sample B [26].

4. Discussion

The essential result shown by figure 4 is the existence of a strong orientation effect of the 211 particles in sample A textured under a magnetic field. The net weakening of the $g_{\parallel}$ component in sample A when $(H, c_{123}) = 90°$ shows that the b_{211} orientation is parallel to c_{123} (symmetrically, the signal for $g_{\parallel}$ is a maximum when $(H, c_{123}) = 0$). According to the x-ray pole figure, figure 3(*b*), the pole $\{040\}_{211}$ is close to the $\{005\}_{123}$ (within less than 10°), which shows that, taking into account the pole dispersion, the direction b_{211} is parallel to c_{123}, a similar conclusion to the one deduced from EPR. It should be underlined that this is the first time a secondary texture for 211 has been detected by x-ray pole figure in textured YBaCuO and that a close agreement for orientations was found between these two very different techniques. A similar observation has been made previously by Pellerin *et al* [17] in textured samples prepared by a modified MTG method. A different orientation was noticed: the b_{211} was found to be located in the (a, b) plane, but the elaboration was not performed in a magnetic field.

All these results point to a possible anisotropy of susceptibility of the 211 precipitates. This last point is in agreement with the orientation of 211 particles in an appropriate fluid under a high magnetic field. The results of this other study which are published elsewhere [27] show the same orientation of the 211 particles with respect to the field.

This fact leads us to wonder about the mechanisms involved during the 123 recrystallization under a magnetic field. Notably, if the 211 particles are oriented by the magnetic field in the peritectic liquid at high temperature, it seems that a substantial part of these 211 particles remains oriented after solidification of the 123 crystal. According to Kobayashi *et al* [20], acicular 211 particles have their long length parallel to the a_{211} axis. As a result of the present study the oriented 211 grains have their long length in the $(a, b)_{123}$ plane after crystallization. It would have been very surprising to have found the long axis perpendicular to the preferential growth direction of $YBa_2Cu_3O_{7-\delta}$ which is along the $(a, b)_{123}$ plane.

Does this particular orientation of the 211 particles induced by the magnetic field play a role in the driving force for the $(a, b)_{123}$ plane alignment and finally impose the growth direction? The answer to these questions will enlighten the understanding of the growth process and experiments are in progress to elucidate them. One should add that probably the 123 nuclei are simultaneously oriented with a tendency to align their c_{123} axis parallel to the applied magnetic field.

On the other hand, does special orientation of 211 grains in 123 textures enhance pinning and favour high J_c? It is especially encouraging in this respect to consider that despite having a fibrous texture, the samples of De

Rango *et al* [7] have high J_c. This could be the result of the special orientation of 211 grains that we might expect in their samples.

5. Conclusion

A sample of 123 + 20% (wt) 211 sol-gel precursor powder has been prepared by unidirectional solidification under a magnetic field. This sample exhibits a single domain about 15 mm in length and 4×4 mm^2 square section. X-ray pole figures show that it is highly textured and its c_{123} axis is almost parallel to the direction of the applied magnetic field.

Orientation of the 211 particles trapped in the 123 matrix has been investigated both by x-ray pole figures and EPR spectroscopy. The main result is that part of the 211 particles have their b_{211} axis parallel with the c_{123} axis when a magnetic field is applied, though no particular orientation is detected when the sample is solidified without a magnetic field.

Experiments, detailed in another publication [27], have confirmed that a magnetic field orientates 211 particles with their b_{211} axis parallel with the direction of the applied magnetic field.

EPR is an excellent probe at the microscopic level, it gives a statistical view of the 211 orientation, contrary to TEM studies.

These results lead us to wonder about the origin of the driving force involved during unidirectional solidification to control the crystal growth direction. The consequences of these observations on the crystallization process are now under investigation.

Acknowledgments

The authors would like to thank Dr D Dierickx from KUL University (Belgium) for supplying the precursor powder. Dr Dierickx is supported by the Belgium High Temperature Impulse Program. This work was partly supported by a co-operative program of CNRS and French Ministère de l'Enseignement Supérieur et de la Recherche Scientifique: Supraconducteurs à Haute Température Critique pour Application en Courants Forts. FJG thanks the European Union for financial support (Human Capital and Mobility).

References

[1] Jin S, Sherwood R C, Gyorgy E R M, Tiefel T H, Van Dover R B, Nakahara S, Shneemeyer L F, Fastnacht R A and Davis M E 1988 *Appl. Phys. Lett.* **52** 2074
[2] Salama K, Selvamanickam V, Gao L and Sun K 1989 *Appl. Phys. Lett.* **54** 2352
[3] Murakami M, Morita M, Doi X and Miyamoto K 1989 *Japan. J. Appl. Phys.* **28** 1189
[4] Salama K and Lee D F 1994 *Supercond. Sci. Technol.* **7** 177
[5] Ferreira J M, Maple M B, Zhou H, Hake R R, Lee B W, Seaman C L, Kuric M V and Guertin R P 1988 *Appl. Phys.* A **47** 402
[6] Farrel D E, Chandrasekhar B S, De Guire M R, Fang M M, Kogan V G, Clem R and Finnemore D K 1987 *Phys. Rev.* B **36** 402
[7] de Rango P, Lees M, Lejay P, Suplice A, Tournier R, Ingold M, Germi P and Pernet M 1991 *Nature* **349** 770
[8] Lee M R, Bourgault D, Braithwaite D, de Rango P, Lejay P, Suplice A and Tournier R 1992 *Physica* C **191** 414
[9] Murakami M 1990 *Mod. Phys. Lett.* B **4** 163
[10] Griffith M L, Hauffman R T and Holloran J W 1994 *J. Mater. Res.* **9** 1633
[11] Durand L and Pastol J L 1994 *Mater. Lett.* **19** 291
[12] Yamamoto T, Chan S K, Lu J G, Prasanna T R S and O'Handley R C 1992 *Phys. Rev.* B **46** 8509
[13] Lee D F, Selvamanickam V and Salama K 1992 *Physica* C **202** 83
[14] Lee D F, Mironova M, Selvamanickam V and Salama K 1992 *Interface Sci.* **1** 381
[15] Wang Z L, Goyal A and Kroeger D M 1993 *Phys. Rev.* B **47** 5373
[16] Ayache J, Odier P and Pellerin N 1994 *Supercond. Sci. Technol.* **7** 655
[17] Pellerin N, Odier P, Simon P and Chateigner D 1994 *Physica* C **222** 133
[18] Vier D *et al* 1987 *Phys. Rev.* B **36** 8888
Mehgeran F 1992 *Phys. Rev.* B **46** 5640
[19] Simon P, Bassat J M, Oseroff S B, Fisk Z, Cheong S W, Wattiaux A and Schultz S 1993 *Phys. Rev.* B **48** 4216
[20] Kobayashi T, Katsuda H, Hayashi K, Tokumoto M T and Ihara H 1988 *Japan. J. Appl. Phys.* **27** L670
[21] Van der Biest O and Kwarciak J 1992 *J. Austr. Ceram. Soc.* **27** 51
[22] Gotor F J, Fert A R, Odier P and Pellerin N *J. Am. Ceram. Soc.* submitted
[23] Schulz L G 1949 *J. Appl. Phys.* **20** 1030
[24] Chateigner D, Germi P and Pernet M 1994 *J. Appl. Crystallogr.* **27** 278
[25] Holland J R 1964 *Adv. X-ray Anal.* **7** 86
[26] Pellerin N unpublished work
[27] Pellerin N, Gotor F J, Simon P, Durand L and Odier P *Solid State Commun.* submitted